

# ChemComm

Accepted Manuscript



This is an *Accepted Manuscript*, which has been through the Royal Society of Chemistry peer review process and has been accepted for publication.

*Accepted Manuscripts* are published online shortly after acceptance, before technical editing, formatting and proof reading. Using this free service, authors can make their results available to the community, in citable form, before we publish the edited article. We will replace this *Accepted Manuscript* with the edited and formatted *Advance Article* as soon as it is available.

You can find more information about *Accepted Manuscripts* in the [Information for Authors](#).

Please note that technical editing may introduce minor changes to the text and/or graphics, which may alter content. The journal's standard [Terms & Conditions](#) and the [Ethical guidelines](#) still apply. In no event shall the Royal Society of Chemistry be held responsible for any errors or omissions in this *Accepted Manuscript* or any consequences arising from the use of any information it contains.

## Nanoparticle-Blood Interactions: The Implications on Solid Tumour Targeting

James Lazarovits,<sup>1,2</sup> Yih Yang Chen,<sup>1,2</sup> Edward A. Sykes<sup>1,2</sup> and Warren C. W. Chan<sup>1-5</sup>

<sup>1</sup>Institute of Biomaterials and Biomedical Engineering, <sup>2</sup>Terrence Donnelly Centre for Cellular and Biomolecular Research, <sup>3</sup>Chemistry, <sup>4</sup>Chemical Engineering, <sup>5</sup>Materials Science and Engineering, University of Toronto, 164 College Street, Toronto, ON, M5S 3G9, Canada

### ***ABSTRACT:***

Nanoparticles are platforms that are well suited for cancer targeting and diagnostic applications. However, on average, less than 5% of all nanoparticles accumulate in the tumour. Here we explore the interactions of blood components with nanoparticles and describe how these interactions influence solid tumour targeting. In the blood, serum proteins adsorb onto nanoparticles to form a protein corona in a manner dependent on nanoparticle physicochemical properties. These serum proteins can block nanoparticle tumour targeting ligands from binding to tumour cell receptors. Additionally, serum proteins can also encourage nanoparticle uptake by macrophages, which decreases nanoparticle availability in the blood and limits tumour accumulation. The formation of this protein corona will also increase nanoparticle hydrodynamic size or induce aggregation, which makes nanoparticles too large to enter the tumour through pores of the leaky vessels, and prevents deep penetration into tumours for cell targeting. Recent studies have focused on developing new chemical strategies to reduce or eliminate serum protein adsorption, and rescue the targeting potential of nanoparticles to tumour cells. An in depth and complete understanding of nanoparticle-blood interactions is key to designing nanoparticles with optimal physicochemical properties with high tumour accumulation. The purpose of this review article is to describe how the protein corona alters the targeting of nanoparticles to solid tumours and explains current solutions to solve this problem.

## ***1. INTRODUCTION:***

Nanotechnology is a rapidly growing field that has captured worldwide attention. Governments and institutions are devoting significant resources to develop nanotechnology-based tools to solve some of the greatest problems in cancer<sup>1,2</sup>. Nanomaterials possess unique optical, electronic, and magnetic properties, and are able to store therapeutic or imaging agents. These properties can be exploited to produce nanoparticles that function as bright contrast agents and as targeted drug delivery vehicles that improve cancer detection and treatment. An example of an FDA approved nanoparticle is Doxil, which is a liposome nanoparticle that is loaded with doxorubicin. It has been shown to significantly increase blood half-life and minimize cardiotoxicity compared to standard doxorubicin treatment<sup>3</sup>. Unfortunately, it is unable to improve patient survival rate<sup>3</sup>. This limited therapeutic efficacy is a trend found across many nanoparticle formulations<sup>4</sup>, and there is insufficient knowledge to explain why these fine-tuned structures do not function as intended. In order to advance cancer nanomedicine, it is crucial to elucidate the reasons behind these discrepancies.

One problem that contributes to this discrepancy is the poor targeting capabilities of nanoparticles. On average, less than 5% of an injected dose accumulates within the tumour<sup>5,6</sup> and it is expected that an even smaller number of nanoparticles will reach the desired cells. Simply injecting more nanoparticles to offset targeting inefficiency will minimally improve therapeutic efficacy, and may result in toxic side effects, as a larger dose of nanoparticles will accumulate in healthy tissues. In order to better understand the factors that affect biodistribution, it is imperative to study the interactions that exist between intravenously injected nanoparticles and the blood, because these interactions change the targeting and transport capabilities of

nanoparticles. In fact, the interactions themselves change as nanoparticles travel through different regions of the body<sup>7-9</sup>. These complex dependencies must be studied in further detail in order to develop solutions to these barriers.

Traditionally, researchers synthesize nanoparticles and subsequently study how their physicochemical characteristics affect cellular and physiological function. It is expected that characteristics such as size, shape, and surface chemistry will dictate nanoparticle behaviour within the body. The first reported speculation of the serum protein effect on nanoparticle cellular interaction was by Chithrani et al using simple protein assays to show gold nanoparticles are coated with serum proteins when introduced into media containing serum<sup>10</sup>. Cedervall et al. then showed that nanoparticles are coated with a diverse population of proteins and they coined the term “protein corona”<sup>11</sup>. Walkey et al. evolved the terminologies to “synthetic identity” and “biological identity” to describe the surface characteristics of the nanoparticles before and after exposure to serum<sup>12</sup>. This field of research has evolved in the last ten years and continues to have interest in the chemistry, materials, engineering, biology, and medical research communities. Fundamental studies of the interface between nanoparticles and serum proteins are important because they have a significant influence on how nanoparticles interact within biological systems. Furthermore, in order to design nanoparticles to function within the body, there is a need to sufficiently design their surfaces to prevent blood-nanoparticle interactions. This requires a full understanding of the mechanisms of nanoparticle-serum protein interaction to develop solutions to mediate these interactions (Figure 1). The lack of knowledge of the interactions of nanoparticles with blood components leads researchers to assume that these interactions inhibit nanoparticle efficacy. However, novel chemical design strategies may

overcome these interactions and enable the nanoparticle to target tissues without interference from blood components. This review will describe the effect of nanoparticle-blood interactions on solid tumour targeting.

## **2. THE BLOOD:**

When nanoparticles are intravenously injected, they first encounter the blood, which is a highly complex fluid composed of both cellular and acellular elements (Figure 2). It maintains pH and temperature, and also facilitates the transport of gases, nutrients, and wastes throughout the body. The cellular portion of the blood contains red blood cells to transport gasses, white blood cells to protect the body against infection, and platelets to close wounds. Conversely, the acellular plasma is composed of 91% water, a small percentage of biomolecules, and a complex concoction of over 1100 unique and multifunctional proteins<sup>13</sup>. When nanoparticles are exposed to the blood, they rapidly attract many different proteins to their surface. These interactions with blood plasma proteins contribute the most to changes in nanoparticle properties such as the aggregation state, surface charge, surface chemistry, and targeting capabilities, which lead to changes in function<sup>14</sup>. Additionally, the cellular and acellular elements will also interact with each other on the nanoparticle surface changes protein conformation, binding affinity, function<sup>7,15-20</sup>, and blood physiology<sup>21,22</sup>. These changes in both blood and nanoparticle properties generates a complex system of biological interactions. This review article will focus on these interactions, but from the perspective of the nanoparticles.

## **3. THE NANOPARTICLE-BLOOD INTERACTIONS:**

**3.1 The Nanoparticle Synthetic Identity:** The ‘synthetic identity’ of a nanoparticle is comprised of its intentionally designed physicochemical properties, which include size, shape, surface chemistry, and surface functionalization. In order to maintain this identity, and ensure monodispersity and biocompatibility in aqueous environments like the blood, researchers coat nanoparticle surfaces with surface passivating groups (i.e. polyethylene glycol [PEG]), and ligands (antibodies, peptides, DNA, or other bio-recognition molecules) that target or react with a cell of interest. Prior to any *in vivo* applications, the synthetic identity is characterized to ensure the quality of the end product. Nanoparticle size and shape are analyzed using electron or atomic force microscopy and the hydrodynamic diameter and surface charge are measured by dynamic light scattering (DLS) and zeta potential. Finally, their dispersity can also be determined using absorbance spectrophotometry, transmission electron microscopy (TEM), DLS, and gel electrophoresis. Nanoparticles are typically used once these characterizations are done, and the “synthetic identity” has been established.

**3.2 The Basis of Protein Corona Formation:** Although it is currently assumed that nanoparticles will present their synthetic identity once injected into the body, the adsorption of blood proteins onto the nanoparticle surface forms a ‘protein corona.’ Protein corona formation is energetically favourable<sup>23,24</sup> and features proteins in low energy state conformations<sup>7,16,19,20,25,26</sup> with stable protein-particle interactions<sup>9</sup>. This structure provides a ‘biological identity’, which increases nanoparticle size by 3-35nm<sup>23,27,28</sup>, and changes the surface charge to -10 to -20mV<sup>24,27</sup>. This biological identity is presented to the body, and can cause unexpected changes in cellular interactions, cellular uptake, biodistribution, and immunogenicity<sup>21,23,30-32</sup>. The overall protein corona profile drives these changes<sup>33</sup>, and

influences nanoparticles to bind to a wide variety of cells<sup>34</sup>. For example, protein coated DOPE-DC cholesterol functionalized liposomes achieve 13-fold increased uptake in PC3 prostate cancer cells<sup>35</sup> compared to uncoated liposomes. Additional examples include non-functionalized, protein-coated liposomes<sup>36</sup>, and iron-oxide nanoparticles<sup>37</sup>, which exhibit 6 and 10 fold increased interaction respectively in isolated liver macrophage cell culture. Improved cellular binding occurs across a wide variety of nanoparticle types and affects a range of biological processes in both harmful and beneficial ways<sup>14,15,34,38-41</sup>. Quantum dots functionalized with DHLA or cysteamine increase in size after exposure to serum proteins, which prevents renal clearance<sup>27</sup>. Additionally, when bare graphene oxide, a generally immunotoxic material, is incubated with 10% fetal bovine serum, ROS production is greatly attenuated and cell viability improves by over 50%<sup>39</sup>. Similarly, the formation of the protein corona on plasma treated silica and polystyrene beads show between 5 and 7-fold increased cell uptake, a major reduction in complement and coagulation pathway activation, and close to 40% increased cell viability<sup>21</sup>.

The composition of the protein corona is influenced by many factors, including the duration of blood exposure<sup>7-9</sup>, the local environment<sup>7-9</sup>, as well as the physicochemical properties<sup>7,18,23,24,26-28,42-57</sup> of nanoparticles themselves. The corona is a temporally dynamic complex<sup>58</sup> whose formation and ultimate structure are governed by protein abundance and binding affinity<sup>18</sup>. Protein coronae composed of low affinity, high abundance proteins<sup>30</sup> are ‘soft’, whereas coronae with high affinity and low abundance proteins are ‘hard’. A soft corona will form on the nanoparticle surface upon intravenous injection. This corona “hardens” over time as low affinity, high abundance proteins are replaced by ones of higher affinity and lower

abundance (Figure 3)<sup>7,9</sup>. In a static environment, it is possible for the corona to reach an equilibrium state<sup>23</sup>, composed of proteins with the highest affinity. However, the composition of blood continuously changes due to convection and cellular metabolism<sup>8,59</sup>, which constantly evolves the protein corona composition (Figure 3). These temporal- and spatial-dependent effects are rarely considered in conventional engineering processes, which assume that biological function is directly related to synthetic identity. To design effective nanoparticles for therapy, the synthetic identity should be tailored to produce a nanoparticle with a desirable biological identity, by taking both the targeted environment<sup>14,23</sup> and the protein corona into consideration.

**3.3 The Relationship Between the Synthetic and Biological Identities:** Although the protein corona and the biological identity determine nanoparticle behaviour within the body, it is possible to design a desirable biological identity using the synthetic identity. While material composition<sup>23,42</sup>, surface chemistry<sup>7,26,43-49</sup>, and shape<sup>24,50</sup> have the most important effects on protein corona composition<sup>42</sup>, other physical properties such size<sup>20,24,25,35,39,41,42,60</sup>, radius of curvature<sup>18,23,26-28,53-55,11</sup>, surface roughness<sup>57</sup>, and hydrophobicity<sup>18,56,11</sup> (Figure 4) (See Table 1) directly impact the biological identity as well. For example, a 200nm silica particle will have an ApoA-1 and serum albumin rich corona, whereas 200nm polystyrene nanoparticles have high levels of fibrinogen- $\alpha/\beta$ <sup>23</sup>. Nanoparticle charge and size change what proteins bind to their surface. Anionic and cationic charged nanoparticles favour proteins with  $pI < 5.5$  and  $pI > 5.5$  respectively<sup>15,42,46</sup>. Smaller nanoparticles with greater curvature favour protein adsorption, because of reduced protein-protein interactions and steric destabilization<sup>7,28</sup>. As size and surface charge change, nanoparticles may begin to repel serum protein, actively bind proteoglycans<sup>44</sup>, or form corona with varying abundances of HDL, LDL, and acute phase proteins<sup>26</sup>. A rougher

surface favours protein adsorption,<sup>57</sup> and increases the potential for cellular interaction<sup>61,62</sup>. The hydrophobicity of the nanoparticle also exerts effects on the protein corona by stabilizing protein binding and encouraging opsonin interaction<sup>63</sup>. For example, more hydrophobic surfaces exhibit greater binding affinity for fibrinogen, whereas less hydrophobic nanoparticles favourably bind serum albumin<sup>18,64</sup>. Increasing the ratio of NIPAM:BAM increases the hydrophobicity of cross-linked copolymer nanoparticles, and will increase protein corona density and change its composition. Cumulatively, all of the properties of the synthetic identity drive protein corona formation, and indirectly dictate *in vivo* nanoparticle behaviour. Knowledge regarding the relationship between these two identities is still sparse, and should be further developed to create design rules that facilitate the creation of more effective targeting nanoparticles.

#### **4. THE INFLUENCE OF BLOOD ON SOLID TUMOUR TARGETING AND CLEARANCE:**

**4.1. Mechanisms of nanoparticle tumour targeting.** Nanoparticles are conventionally injected into animals where they circulate in the blood, and if they are small enough, they will extravasate into tumours through the pores of blood vessels and are retained within the tumour tissue for a certain period of time. This process is known as the enhanced permeability and retention (EPR) effect. The mechanism of particle retention in a tumour is dependent on whether the nanoparticle is designed for a passive or active targeting mechanism (Figure 5). In passive targeting, nanoparticles enter the tumour via the leaky vasculature that is formed when cancerous tissues undergo rapid vascularization<sup>65</sup>. This process leads to large pores in the vessel walls (~200 nm, depending on the stage and type of tumour) that allow foreign materials to diffuse into the tumour milieu<sup>66</sup>. For this process, a nanoparticle is commonly coated with the polymer PEG

that prevents its uptake by cells of the reticuloendothelial system (macrophages and dendritic cells) and allows for long circulation in the blood<sup>24,67</sup>.

Passive targeting is usually limited by the diffusion of the agent into and out of the tumour. In contrast, for active targeting, the nanoparticle surface is coated with molecules or ligands that bind to endothelial cells on the tumour vessels, in the tumour site (e.g., extracellular matrix), on the surface of cancer cells, or inside the cancer cells<sup>68</sup>. While the EPR effect has driven the development of many nanotechnologies, the EPR effect is becoming a controversial concept in nanoparticle targeting because its presence across different species has yet to be established. Additionally, an EPR-based nanoparticle tumour targeting theory simplifies the effects of tumour and tissue heterogeneity, tumour architecture, differential tissue perfusion, hemodynamic regulation, and lymphogenesis<sup>4</sup> on nanoparticle biodistribution. This theory also neglects the importance of blood-nanoparticle interactions, which plays an active role in nanoparticle behaviour.

**4.2 How does nanoparticle-blood interaction influence tumour targeting?** There are several mechanisms that describe the influence of blood components on nanoparticle tumour targeting. (1) Serum proteins adsorb onto the surface of active targeting nanoparticles and block the bio-recognition molecule from binding to the tumour cell receptor<sup>6</sup>. (2) Nanoparticle surfaces are not coated with a high enough density or long-enough anti-fouling polymer (a threshold unique for each nanoparticle type), which encourages blood protein adsorption, which induces nanoparticles to be taken up by macrophages<sup>24,67</sup>. (3) Serum blood protein adsorption and small ions causes an increase in overall hydrodynamic size and/or nanoparticle aggregation, which

increases macrophage uptake rate and decrease the ability to enter and/or penetrate into the tumour<sup>21</sup>.

**4.2a Serum proteins block nanoparticle active targeting.** Nanoparticles are commonly synthesized to target cells via a passive or an active targeting mechanism. Active targeting relies on surface-functionalized ligands, which bind to cell-surface receptors to induce receptor-mediated endocytosis and increase tissue-retention<sup>69,70</sup>. Nanoparticles functionalized with antibodies, peptide sequences, oligonucleotides<sup>71</sup>, and polyelectrolytes can trigger protein-signaling cascades, induce cell uptake through receptor-mediated endocytosis<sup>72-74</sup>, and target sub-cellular organelles and molecules<sup>75</sup> (Figure 5a). However, the presence and formation of a protein corona at the nanoparticle surface will cause new interactions with off-target cells and deviate the nanoparticle from its intended target<sup>6,46</sup> (Figure 5b). Serum protein adsorption to nanoparticles coated with targeting ligands may block bio-recognition molecules from binding to the target receptor through steric effects<sup>6,76</sup>. This can occur when the surface of nanoparticles are not coated with a high enough density of the targeting molecule. The uncoated surface can adsorb to the serum protein and the protein corona can mask the nanoparticle surface by sterically hindering receptor access to targeting ligands, and inhibit nanoparticle targeting capabilities by decreasing the probability of a favourable receptor-ligand binding event<sup>4</sup>. Additionally, the protein corona could potentially force a premature release of the drug payload via ligand exchange, in which the stability and integrity of the nanoparticle is disrupted due to protein corona interference with surface-adsorbed ligands, thereby severely diminishing therapeutic efficacy<sup>77</sup>.

**4.2b Serum protein adsorption affects passive targeting.** In passive targeting, nanoparticles are typically coated with anti-fouling polymers such as PEG. These polymers are hydrophilic and have near neutral charges. When these passive targeting nanoparticles are designed, they tend to have longer blood half-lives because serum proteins interactions are mostly eliminated, thus preventing macrophages from recognizing the nanoparticles (Figure 5c)<sup>24,67,78</sup>. However, it has recently been shown that the density and length of the anti-fouling polymer on the surface of nanoparticles determines the efficiency of preventing protein-nanoparticle interaction. To reduce serum protein adsorption and macrophage uptake, Walkey *et al.* and Yang *et al.* showed that gold and polystyrene nanoparticles require a PEG-polymer that is larger than 5 kDa with a density of  $\sim 0.64$  PEG/nm<sup>2</sup>, and a 2 kDa PEG with a density of  $\sim 1$  PEG/nm<sup>2</sup>, respectively<sup>21,62</sup>. Others have noted that the greatest reduction of non-specific serum protein adsorption occurs at an optimal surface density, in which the PEG conformation on the nanoparticle surface is at an intermediate conformation between the ‘mushroom’ to ‘brush’ configuration<sup>79,80</sup>. Optimizing the surface density and length of PEG on nanoparticle surfaces effectively minimizes macrophage-nanoparticle interactions (Figure 6)<sup>67</sup>. Interestingly, the PEG density and length also determines the type of serum proteins adsorbed to the nanoparticle surface. It remains unclear how the differences and diversities of these serum proteins influence their *in vivo* trajectory and cellular binding. Nevertheless, these studies demonstrate the importance of nanoparticle surface design in avoiding serum protein adsorption and macrophage sequestration.

**4.2c The influence of nanoparticle size in mediating tumour accumulation.** The transport of nanoparticles into the tumour is heavily dependent on nanoparticle size. The leaky vessels in the

tumour vasculature have pores that range in size from 50 to 500nm, which depend on the stage and type of tumour<sup>81</sup>. Nanoparticles over the optimal tissue penetration diameter of 30-60nm<sup>25</sup> internalize slower<sup>82</sup>, exhibit delayed diffusion kinetics<sup>83</sup> and altered surface charge density<sup>24,29</sup>. Metal nanoparticles with core diameter larger than 100nm are found near the blood vessel and do not appear to penetrate into the tumour<sup>84</sup>. Once nanoparticles enter the tumour, they will need to penetrate into the tumour for it to target the cells. The rate of movements of nanoparticles through tumours also depends on size<sup>85</sup>.

Nanoparticles that acquire a protein corona exhibit an increased hydrodynamic diameter<sup>25,82,86</sup>, and change shape<sup>16,17,24</sup> and charge<sup>24,86</sup>, which leads to unexpected changes in tumour accumulation (Figure 5d). Nanoparticles can aggregate in the presence of serum protein<sup>87</sup>, and this increase in size impedes their penetration into tumours, and increase their chances to be taken by macrophages (as macrophages prefer to take up larger structures). There must be more investigations into this relationship, since these protein corona-induced changes in physicochemical parameters can potentially limit extravasation and penetration of nanoparticles in tumours as well as encourage clearance from the blood by macrophage uptake.

**4.3 Current 'solutions' to the problem.** While the influence of the protein corona on targeting is clear, researchers are now starting to focus on developing solutions to this potential problem. The problem is likely to due to a chemistry design issue, where the nanoparticles' surface is not sufficiently coated with the optimal type, or density of molecules to resist non-specific protein adsorption. Consequently, the nanoparticle surface would have space for serum proteins to adsorb and build a corona. Two solutions have been recently proposed: (a) the backfilling of antibody-coated nanoparticles with smaller 1 kDa methoxy terminated PEG to fill spaces on the

nanoparticle surface that minimizes serum proteins from binding<sup>73</sup>. And, (b) coating of nanoparticle surface with benzyl moieties to make the nanoparticle resistant to protein binding<sup>76</sup>. Specifically, it has been demonstrated that serum protein adsorption on Herceptin conjugated gold nanoparticles is drastically reduced after back-filling the leftover bare nanoparticle surfaces with small 1 kDa methoxy terminated PEG. This method does not reduce targeting specificity, and improves receptor-mediated nanoparticle binding by two to five fold compared to unpassivated, and 5 and 10 kDa pegylated nanoparticles<sup>88</sup>. Alternatively, aromatically functionalized cationic gold nanoparticles<sup>76</sup> with careful manipulation of electron withdrawing or donating benzyl moieties can also reduce unwanted protein interactions. In both cases, neither surface passivation method can completely eliminate nanoparticle-protein interactions<sup>89,90</sup> but were good enough to minimize serum protein adsorption and enable cellular targeting. Further investigation on the *in vivo* behaviour of nanoparticles with these new surface chemistries are required to determine whether these designs improve tumour-targeting efficiency. Nevertheless, an opportunity exists for researchers to focus on better surface chemical designs to reduce protein corona formation and macrophage uptake, in order to improve tumour cell targeting.

##### **5. THE INTERACTIONS OF NANOPARTICLES WITH CIRCULATING BLOOD CELLS.**

The formation of the protein corona changes the presented identity of the nanoparticle and can trigger responses from circulating blood cells. Upon intravenous administration, opsonins - a class of blood proteins composed of non-specific antibodies and complement proteins - bind to the nanoparticle surface and flag nanoparticles as foreign entities<sup>91</sup>. Within minutes<sup>5</sup> following intravenous administration, erythrocytes<sup>92</sup>, and resident phagocytes such as

macrophages, monocytes, granulocytes and dendritic cells<sup>93–97</sup> engulf and phagocytose nearly 95% of the injected dose and prevent them from reaching the tumour<sup>24</sup>.

In addition to the effect of the corona on nanoparticle circulation, the interactions of nanoparticles with blood cells may also influence their ability to target tumours and tumour cells. Smith *et al.* physisorbed CY5.5 onto the surface of single-walled carbon nanotubes and injected them into tumour-bearing mice and showed using flow cytometry that a subset of non-neutrophil circulating monocytes, which represent only 3% of all blood cells, showed nearly 100% uptake of the injected dose (Figure 7)<sup>98</sup>. Although specific nanoparticle-blood interactions cannot be derived from this data, nanoparticles are shown to be delivered to the tumour through these monocytes, independent of the EPR effect. In another study, Bischof and co-worker showed that white blood cells were able to uptake 30 nm gold nanoparticles *ex vivo*, but were unable to uptake the nanoparticles *in vivo*<sup>99</sup>. A difference in the results may be due that the fact that nanoparticles are in flow *in vivo* while they are stagnant *ex vivo*. While there needs to be further studies on blood cell nanoparticle-interactions, we can speculate that circulating phagocytic cells may take up the nanoparticles in transit in the blood. Essentially this reduces the amount of nanoparticles available for tumour targeting.

## 6. DISCUSSION:

Advancements in nanotechnology have led to the development of many different types of nanoparticles for cancer therapy. However, there is a general lack of clinical efficacy of these nanoparticles *in vivo*. Although these nanoparticles have been extensively characterized and designed to target tumours, the large amount of off-target accumulation cannot be ignored. For this reason, the biological environments that interact with the nanoparticles en route to the

tumour must be examined with closer scrutiny. The first such environment is the blood, and it has been demonstrated many times in this review that blood proteins will change a nanoparticle's presented identity by adsorbing to the nanoparticle surface. To better understand the ramifications of the biological identity on nanoparticle biodistribution and tumour targeting efficacy, there is a need to link the synthetic characteristics of each type of nanoparticle to its protein corona composition, and the resultant biodistribution pattern. In order to achieve this, a database will likely need to be developed for serum protein-to-nanoparticle interactions. The adsorption of serum proteins on different nanoparticles should be identified with different biological function (e.g., cell uptake and biodistribution). This database will allow the use of QSAR (Quantitative Structure Activity Relationship) methods to correlate the synthetic identity, biological identity, and cellular behaviour. This will enable the prediction of biological function based on nanoparticle design. Without this large database set, it will be difficult to correlate these nano-bio relationships.

In 2014, Walkey and colleagues developed the first example of such a database. They investigated over 80 different gold nanoparticle designs to develop a QSAR model using nanoparticle fingerprints to predict cellular interactions. Nanoparticle fingerprints are derived from corona protein composition and abundance heat maps using liquid chromatography tandem mass spectroscopy (Figure 8). Their work showed that material composition, surface chemistry, and size have the greatest influence on protein corona structure. For example, when exposed to a constant serum source, gold and silver nanoparticles of the same size and charge differ in protein corona composition by 63.1%. Cationic amine and anionic carboxy functionalized gold nanoparticles acquire protein

coronae that differ in composition by 52.8%. Finally, 15nm and 30nm gold nanoparticles differ by 25.3%, whereas 30nm and 60nm gold nanoparticles differ by 13.3%. This library of nanoparticle fingerprints led to the development of a QSAR model that was used to predict the binding capacity of hyaluronan-functionalized nanoparticle to A549 cells. Alone, the QSAR model achieved 50% more predictive power than standard characterization methods, such as DLS, zeta potential, TEM and absorbance spectrophotometry. However, when these two models were used in tandem, accuracy significantly improved ( $Q^2_{LOO}$  of 0.86). Interestingly, in this study, the researchers showed that protein fingerprinting of gold nanoparticle cannot predict how other particle types associate with cells. This suggests the need to create libraries of serum protein interactions with different nanoparticle types (Figure 9). This would lead to a complete database of nanoparticle-serum protein interactions that can be used to predict nano-bio interactions. Nevertheless, this study shows how the biological identity has a direct effect on cellular interaction<sup>42</sup>, and its effects can be simulated using computer modelling techniques. Other researchers are starting to adapt this research strategy to study the protein corona on liposomes.<sup>99</sup>

The development of a nanoparticle protein corona database would be an extremely beneficial tool for nanoparticle research. By building this database, it may be possible to predict the composition of the protein corona on a nanoparticle in a certain biological system, and determine how this specific protein corona will affect the biodistribution of the nanoparticle. These predictions could lead to the development of more efficient drug delivery vehicles. The work performed by Smith *et al.* showed carbon nanotube uptake by a specific population of monocytes<sup>98</sup>. If this behaviour can be pinpointed to a set of proteins within the corona of the

nanotube, it may be possible to target these monocytes by grafting these specific proteins onto other nanoparticles, or be extended to target other cell populations. This database could also be used to associate specific nanoparticle characteristics with specific blood proteins. Furthermore, these associations between the synthetic identity and biological identity could allow researchers to rationally engineer nanoparticles to specifically target tumours and avoid off-target organs.

There is contentious debate surrounding the importance of the protein corona. Some argue that it is a constant occurrence, whereas others believe it is the result of ineffective design. This database may show that protein interaction is a by-product of misguided synthesis and not the result of an uncontrollable natural phenomenon. In any case, many areas of nanomedicine could be dramatically improved if the interplay between the physicochemical properties of nanoparticles, the protein corona composition, and the subsequent biological behaviour of the nanoparticles are empirically determined. A concerted global effort is required to build this database, and take the next leap in the development of nanotechnology for cancer applications.

## **ACKNOWLEDGEMENTS**

The authors would like to acknowledge the Canadian Institute of Health Research, Natural Sciences and Engineering Research Council for their funding support.

**REFERENCE:**

1. M. C. Roco, *National Nanotechnology Investment in the FY 2015 Budget*, 2014.
2. T. Harper, *Global Funding Of Nanotechnologies & Its Impact*, London, 2011.
3. M. E. R. O'Brien, N. Wigler, M. Inbar, R. Rosso, E. Grischke, A. Santoro, R. Catane, D. Kieback, P. Tomczak, S. Ackland, F. Orlandi, L. Mellars, L. Alland, and C. Tendler, *Ann. Oncol.*, 2004, **15**, 440–449.
4. N. Bertrand, J. Wu, X. Xu, N. Kamaly, and O. C. Farokhzad, *Adv. Drug Deliv. Rev.*, 2014, **66**, 2–25.
5. Y. H. Bae and K. Park, *J. Control. Release*, 2012, **153**, 198–205.
6. V. Mirshafiee, M. Mahmoudi, K. Lou, J. Cheng, and M. L. Kraft, *Chem. Commun. (Camb)*, 2013, **49**, 2557–9.
7. E. Casals, T. Pfaller, A. Duschl, G. J. Oostingh, and V. Puentes, *ACS Nano*, 2010, **4**, 3623–32.
8. M. Lundqvist, J. Stigler, T. Cedervall, T. Berggård, M. B. Flanagan, I. Lynch, G. Elia, and K. Dawson, *ACS Nano*, 2011, **5**, 7503–9.
9. D. Dell'Orco, M. Lundqvist, C. Oslakovic, T. Cedervall, and S. Linse, *PLoS One*, 2010, **5**, e10949.
10. B. D. Chithrani, A. a Ghazani, and W. C. W. Chan, *Nano Lett.*, 2006, **6**, 662–8.
11. T. Cedervall, I. Lynch, S. Lindman, T. Berggård, E. Thulin, H. Nilsson, K. a Dawson, and S. Linse, *Proc. Natl. Acad. Sci. U. S. A.*, 2007, **104**, 2050–5.
12. S. D. Perrault, C. Walkey, T. Jennings, H. C. Fischer, and W. C. W. Chan, *Nano Lett.*, 2009, **9**, 1909–15.
13. N. L. Anderson, M. Polanski, R. Pieper, T. Gatlin, R. S. Tirumalai, T. P. Conrads, T. D. Veenstra, J. N. Adkins, J. G. Pounds, R. Fagan, and A. Lobley, *Mol. Cell. Proteomics*, 2004, **3**, 311–26.

14. A. M. Alkilany, P. K. Nagaria, C. R. Hexel, T. J. Shaw, C. J. Murphy, and M. D. Wyatt, *Small*, 2009, **5**, 701–8.
15. K. Prapainop, D. P. Witter, and P. Wentworth, *J. Am. Chem. Soc.*, 2012, **134**, 4100–3.
16. S. Kittler, C. Greulich, J. S. Gebauer, J. Diendorf, L. Treuel, L. Ruiz, J. M. Gonzalez-calbet, and M. Vallet-, *J. Mater. Chem.*, 2010, 512–518.
17. J. E. Schnitzer, A. Sung, R. Horvat, and J. Bravo, *J. Biol. Chem.*, 1992, **267**, 24544–24553.
18. T. Cedervall, I. Lynch, M. Foy, T. Berggård, S. C. Donnelly, G. Cagney, S. Linse, and K. a Dawson, *Angew. Chem. Int. Ed. Engl.*, 2007, **46**, 5754–6.
19. A. A. Vertegel, R. W. Siegel, and J. S. Dordick, *Langmuir*, 2004, **20**, 6800–6807.
20. C. E. Rodriguez, J. M. Fukuto, K. Taguchi, J. Froines, and A. K. Cho, *Chem. Biol. Interact.*, 2005, **155**, 97–110.
21. S. Tenzer, D. Docter, J. Kuharev, A. Musyanovych, V. Fetz, R. Hecht, F. Schlenk, D. Fischer, K. Kiouptsi, C. Reinhardt, K. Landfester, H. Schild, M. Maskos, S. K. Knauer, and R. H. Stauber, *Nat. Nanotechnol.*, 2013, **8**, 772–81.
22. M. Poirier, J.-C. Simard, F. Antoine, and D. Girard, *J. Appl. Toxicol.*, 2014, **34**, 404–12.
23. M. P. Monopoli, D. Walczyk, A. Campbell, G. Elia, I. Lynch, F. B. Bombelli, and K. a Dawson, *J. Am. Chem. Soc.*, 2011, **133**, 2525–34.
24. C. D. Walkey, J. B. Olsen, H. Guo, A. Emili, and W. C. W. Chan, *J. Am. Chem. Soc.*, 2012, **134**, 2139–47.
25. A. E. Nel, L. Mädler, D. Velegol, T. Xia, E. M. V Hoek, P. Somasundaran, F. Klaessig, V. Castranova, and M. Thompson, *Nat. Mater.*, 2009, **8**, 543–57.
26. M. Lundqvist, J. Stigler, G. Elia, I. Lynch, T. Cedervall, and K. a Dawson, *Proc. Natl. Acad. Sci. U. S. A.*, 2008, **105**, 14265–70.
27. H. S. Choi, W. Liu, P. Misra, E. Tanaka, J. P. Zimmer, B. Itty Ipe, M. G. Bawendi, and J. V Frangioni, *Nat. Biotechnol.*, 2007, **25**, 1165–70.
28. M. a Dobrovolskaia, A. K. Patri, J. Zheng, J. D. Clogston, N. Ayub, P. Aggarwal, B. W. Neun, J. B. Hall, and S. E. McNeil, *Nanomedicine*, 2009, **5**, 106–17.
29. G. W. Doorley and C. K. Payne, *Chem. Commun. (Camb.)*, 2011, **47**, 466–8.

30. D. Walczyk, F. B. Bombelli, M. P. Monopoli, I. Lynch, and K. a Dawson, *J. Am. Chem. Soc.*, 2010, **132**, 5761–8.
31. Y. Hong, J. W. Y. Lam, and B. Z. Tang, *Chem. Soc. Rev.*, 2011, **40**, 5361–88.
32. M. P. Monopoli, C. Aberg, A. Salvati, and K. a Dawson, *Nat. Nanotechnol.*, 2012, **7**, 779–86.
33. D. Simberg, J.-H. Park, P. P. Karmali, W.-M. Zhang, S. Merkulov, K. McCrae, S. N. Bhatia, M. Sailor, and E. Ruoslahti, *Biomaterials*, 2009, **30**, 3926–33.
34. M. Clift, S. Bhattacharjee, D. Brown, and V. Stone, *Toxicol. Lett.*, 2010, **198**, 358–365.
35. A. L. Barrán-Berdón, D. Pozzi, G. Caracciolo, A. L. Capriotti, G. Caruso, C. Cavaliere, A. Riccioli, S. Palchetti, and A. Laganà, *Langmuir*, 2013, **29**, 6485–94.
36. J. T. P. Derksen, H. W. M. Morselt, D. Kalicharan, C. Hulstaert, and G. Scherphof, *Exp. Cell Res.*, 1987, **168**, 105–115.
37. A. Beduneau, Z. Ma, C. B. Grotepas, A. Kabanov, B. E. Rabinow, N. Gong, R. L. Mosley, H. Dou, M. D. Boska, and H. E. Gendelman, *PLoS One*, 2009, **4**, 1–12.
38. M. J. D. Clift, M. S. P. Boyles, D. M. Brown, and V. Stone, *Nanotoxicology*, 2010, **4**, 139–49.
39. W. Hu, C. Peng, M. Lv, X. Li, Y. Zhang, N. Chen, C. Fan, and Q. Huang, *ACS Nano*, 2011, **5**, 3693–700.
40. N. P. Mortensen, G. B. Hurst, W. Wang, C. M. Foster, P. D. Nallathamby, and S. T. Retterer, *Nanoscale*, 2013, **5**, 6372–80.
41. G. M. Mortimer, N. J. Butcher, A. W. Musumeci, Z. J. Deng, D. J. Martin, and R. F. Minchin, *ACS Nano*, 2014, **8**, 3357–66.
42. C. D. Walkey, J. B. Olsen, F. Song, R. Liu, H. Guo, W. Olsen, Y. Cohen, A. Emili, and W. C. W. Chan, *ACS Nano*, 2014, **8**, 2439–2455.
43. D. Hühn, K. Kantner, C. Geidel, S. Brandholt, I. De Cock, S. J. H. Soenen, P. Rivera Gil, J.-M. Montenegro, K. Braeckmans, K. Müllen, G. U. Nienhaus, M. Klapper, and W. J. Parak, *ACS Nano*, 2013, **7**, 3253–63.
44. C. Fleischer and C. Payne, *J. Phys. Chem. B*, 2012, **116**, 8901–7.
45. F. Benetti, M. Fedel, L. Minati, G. Speranza, and C. Migliaresi, *J. Nanoparticle Res.*, 2013, **15**, 1694–1703.

46. G. Caracciolo, F. Cardarelli, D. Pozzi, F. Salomone, G. Maccari, G. Bardi, A. L. Capriotti, C. Cavaliere, M. Papi, and A. Laganà, *ACS Appl. Mater. Interfaces*, 2013, **5**, 13171–9.
47. R. Podila, R. Chen, P. C. Ke, J. M. Brown, and a M. Rao, *Appl. Phys. Lett.*, 2012, **101**, 263701–4.
48. a Gessner, R. Waicz, a Lieske, B. Paulke, K. Mäder, and R. H. Müller, *Int. J. Pharm.*, 2000, **196**, 245–9.
49. A. L. Capriotti, G. Caracciolo, C. Cavaliere, P. Foglia, D. Pozzi, R. Samperi, and A. Laganà, *J. Proteomics*, 2012, **75**, 1924–32.
50. C. Röcker, M. Pötzl, F. Zhang, W. J. Parak, and G. U. Nienhaus, *Nat. Nanotechnol.*, 2009, **4**, 577–80.
51. S. Tenzer, D. Docter, S. Rosfa, A. Wlodarski, A. Rekik, S. K. Knauer, C. Bantz, T. Nawroth, C. Bier, J. Sirirattanapan, W. Mann, L. Treuel, R. Zellner, M. Maskos, and R. H. Stauber, *ACS Nano*, 2011, **5**, 7155–7167.
52. H. Zhang, K. Burnum, and M. Luna, *Proteomics*, 2011, **11**, 4569–4577.
53. J. E. Gagner, M. D. Lopez, J. S. Dordick, and R. W. Siegel, *Biomaterials*, 2011, **32**, 7241–52.
54. S. Goy-López, J. Juárez, M. Alatorre-Meda, E. Casals, V. F. Puentes, P. Taboada, and V. Mosquera, *Langmuir*, 2012, **28**, 9113–26.
55. P. Roach, D. Farrar, and C. C. Perry, *J. Am. Chem. Soc.*, 2006, **128**, 3939–45.
56. T. Blunk, D. F. Hochstrasser, J. C. Sanchez, B. Muller, and R. Muller, *Electrophoresis*, 1993, **14**, 1382–1387.
57. E. M. V Hoek and G. K. Agarwal, *J. Colloid Interface Sci.*, 2006, 298, 50–8.
58. L. Vroman and A. L. Adams, *Surf. Sci.*, 1969, **16**, 438–446.
59. G. Maiorano, S. Sabella, B. Sorce, V. Brunetti, M. A. Malvindi, R. Cingolani, and P. P. Pompa, *ACS Nano*, 2010, **4**, 7481–91.
60. S. Zhang, J. Li, G. Lykotrafitis, G. Bao, and S. Suresh, *Adv. Mater.*, 2009, **21**, 419–424.
61. M. S. Ehrenberg, A. E. Friedman, J. N. Finkelstein, G. Oberdörster, and J. L. McGrath, *Biomaterials*, 2009, **30**, 603–10.

62. B. J. Crielaard, a Yousefi, J. P. Schillemans, C. Vermehren, K. Buyens, K. Braeckmans, T. Lammers, and G. Storm, *J. Control. Release*, 2011, **156**, 307–14.
63. C. Gunawan, M. Lim, C. P. Marquis, and R. Amal, *J. Mater. Chem. B*, 2014, **2**, 2060–2083.
64. D. Dell’Orco, *J. Nanomedicine. Biotherapeutic Discov.*, 2012, **02**, 1–2.
65. A. K. Iyer, G. Khaled, J. Fang, and H. Maeda, *Drug Discov. Today*, 2006, **11**, 812–8.
66. K. Maruyama, T. Yuda, a Okamoto, S. Kojima, a Suginaka, and M. Iwatsuru, *Biochim. Biophys. Acta*, 1992, **1128**, 44–9.
67. Q. Yang, S. W. Jones, C. L. Parker, W. C. Zamboni, J. E. Bear, and S. K. Lai, *Mol. Pharm.*, 2014, **11**, 1250–8.
68. T. M. Allen and P. R. Cullis, *Science*, 2004, **303**, 1818–22.
69. O. C. Farokhzad and R. Langer, *ACS Nano*, 2009, **3**, 16–20.
70. A. Salvati, A. S. Pitek, M. P. Monopoli, K. Prapainop, F. B. Bombelli, D. R. Hristov, P. M. Kelly, C. Åberg, E. Mahon, and K. a Dawson, *Nat. Nanotechnol.*, 2013, **8**, 137–43.
71. D. Giljohann, D. Seferos, and P. Patel, *Nano ...*, 2007, **8**, 3818–3121.
72. M. Sun, L. Yang, P. Jose, L. Wang, and J. Zweit, *J. Mater. Chem. B*, 2013, **1**, 6137–6146.
73. H. Chen, H. Paholak, M. Ito, K. Sansanaphongpricha, W. Qian, Y. Che, and D. Sun, *Nanotechnology*, 2013, **24**, 1–9.
74. S. E. A. Gratton, P. A. Ropp, P. D. Pohlhaus, J. C. Luft, V. J. Madden, M. E. Napier, and J. M. Desimone, *Proc. Natl. Acad. Sci. U. S. A.*, 2008, **105**, 11613–11618.
75. P. M. Valencia, E. M. Pridgen, B. Perea, S. Gadde, C. Sweeney, P. W. Kantoff, N. H. Bander, S. J. Lippard, R. Langer, R. Karnik, and O. C. Farokhzad, *Nanomedicine (Lond.)*, 2013, **8**, 687–98.
76. S. D. Conner and S. L. Schmid, *Nature*, 2003, **422**, 37–44.
77. Y. Li, M. S. Budamagunta, J. Luo, W. Xiao, J. C. Voss, and K. S. Lam, *ACS Nano*, 2012, **6**, 9485–95.
78. C. D. Walkey and W. C. W. Chan, *Chem. Soc. Rev.*, 2012, **41**, 2780–99.
79. D. E. Owens and N. a Peppas, *Int. J. Pharm.*, 2006, **307**, 93–102.

80. H. Du, P. Chandaroy, and S. W. Hui, *Biochim. Biophys. Acta*, 1997, **1326**, 236–48.
81. F. Yuan, M. Dellian, D. Fukumura, M. Leunig, D. A. Berk, V. P. Torchilin, and R. K. Jain, 1995, 3752–3756.
82. P. Decuzzi, B. Godin, T. Tanaka, S.-Y. Lee, C. Chiappini, X. Liu, and M. Ferrari, *J. Control. Release*, 2010, **141**, 320–7.
83. B. D. Chithrani and W. C. W. Chan, *Nano Lett.*, 2007, **7**, 1542–50.
84. E. A Sykes, J. Chen, G. Zheng, and W. C. W. Chan, *ACS Nano*, 2014, **8**, 5696–706.
85. W. Jiang, B. Y. S. Kim, J. T. Rutka, and W. C. W. Chan, *Nat. Nanotechnol.*, 2008, **3**, 145–50.
86. Y. Zhao, X. Sun, G. Zhang, B. G. Trewyn, I. I. Slowing, and V. S. Lin, *ACS Nano*, 2011, **5**, 1366–1375.
87. A. Albanese, C. D. Walkey, J. B. Olsen, H. Guo, A. Emili, W. C. W. Chan, *ACS Nano*, 2014, **8**, 5515–5526.
88. Q. Dai, C. Walkey, and W. C. W. Chan, *Angew. Chem. Int. Ed. Engl.*, 2014, **53**, 5093–6.
89. R. Gref, M. Lück, P. Quellec, M. Marchand, E. Dellacherie, S. Harnisch, T. Blunk, and R. Müller, *Colloids Surf. B. Biointerfaces*, 2000, **18**, 301–313.
90. L. D. Unsworth, H. Sheardown, and J. L. Brash, *Langmuir*, 2008, **24**, 1924–9.
91. K. Murphy, *Janeway's Immunobiology*, Garland Science, New York, 8th edn., 2012.
92. B. M. Rothen-Rutishauser, S. Schürch, B. Haenni, N. Kapp, and P. Gehr, *Environ. Sci. Technol.*, 2006, **40**, 4353–9.
93. R. Kedmi, N. Ben-Arie, and D. Peer, *Biomaterials*, 2010, **31**, 6867–75.
94. A. E. Porter, M. Gass, J. S. Bendall, K. Muller, A. Goode, J. N. Skepper, P. a Midgley, and M. Welland, *ACS Nano*, 2009, **3**, 1485–92.
95. D. Baumann, D. Hofmann, S. Nullmeier, P. Panther, C. Dietze, A. Musyanovych, S. Ritz, K. Landfester, and V. Mailänder, *Nanomedicine (Lond.)*, 2013, **8**, 699–713.
96. H. Salik, V. Jeroen, and peter H. M. Hoet, *Int. J. Nanomedicine*, 2012, **7**, 4571–4580.
97. G. Didenko, S. Prylutska, Y. Kichmarenko, G. Potebnya, Y. Prylutsky, N. Slobodyanik, U. Ritter, and P. Scharff, *Materwiss. Werksttech.*, 2013, **44**, 124–128.

98. B. R. Smith, E. E. B. Ghosn, H. Rallapalli, J. a Prescher, T. Larson, L. a Herzenberg, and S. S. Gambhir, *Nat. Nanotechnol.*, 2014, **9**, 481–7.
99. N. B. Shah, G. M. Vercellotti, J. G. White, A. Fegan, C. R. Wagner, and J. C. Bischof, *Mol. Pharm.*, 2012, **9**, 2146–55.

**FIGURES:**

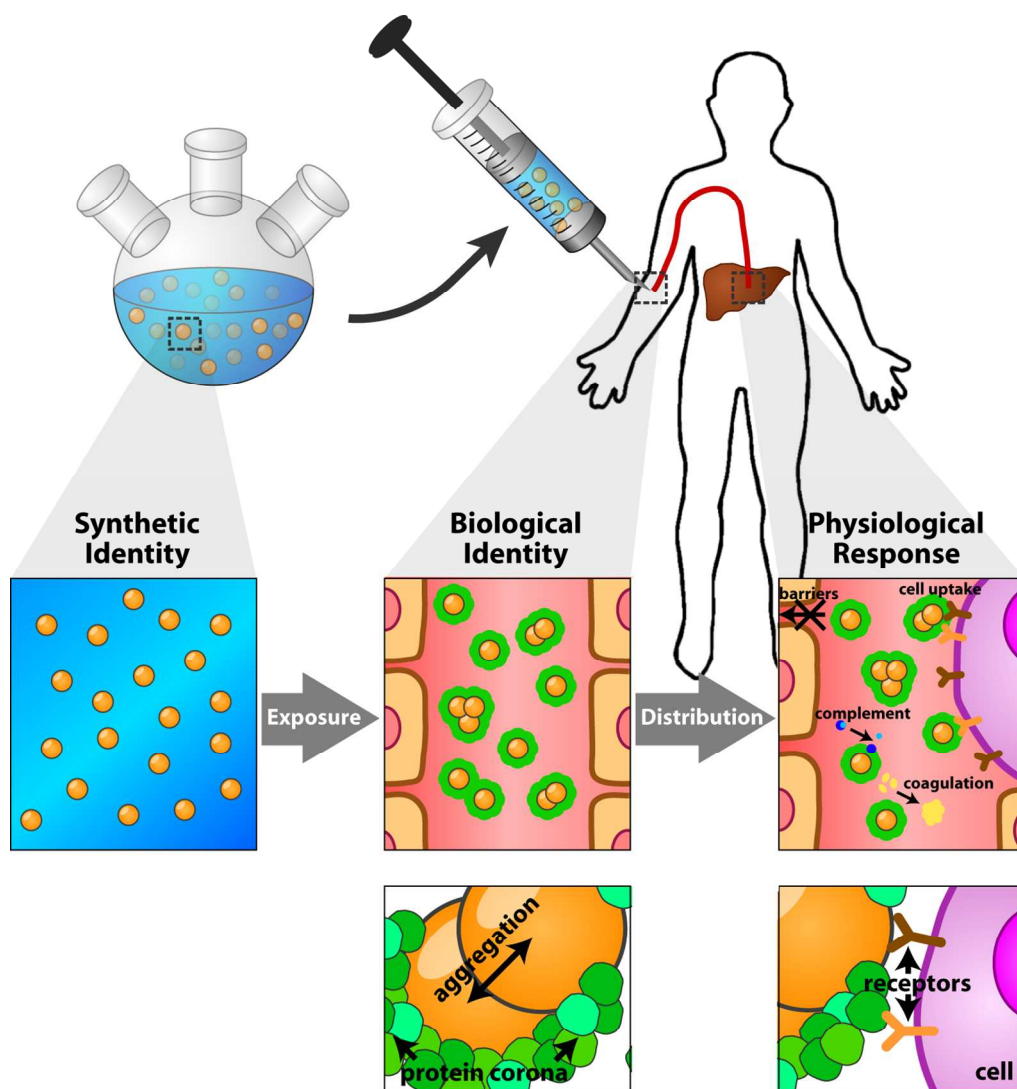


**Figure 1: Blood-nanoparticle interactions change nanoparticle identity and affect physiological responses.** When nanoparticles are injected intravenously, blood proteins bind to the surface and form a protein corona. The proteins bound to the surface provide the nanoparticles with a biological identity, which changes its interactions with cells, biological barriers and the body (figure taken from Walkey *et al.* 2012 with permission)<sup>78</sup>.

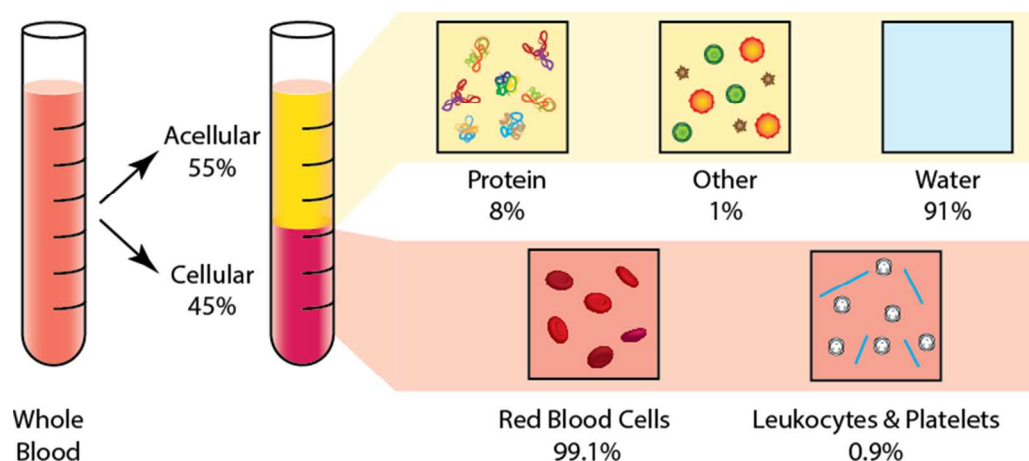


**Figure 2: The molecular composition of whole blood.** The molecular composition of whole blood can be broken down into its acellular and cellular elements. The acellular plasma contains 91% water, a small percentage of biomolecules, and a complex concoction of over 1100 unique and multifunctional proteins. The cellular elements contain primarily red blood cells and less than one percent white blood cells and platelets.

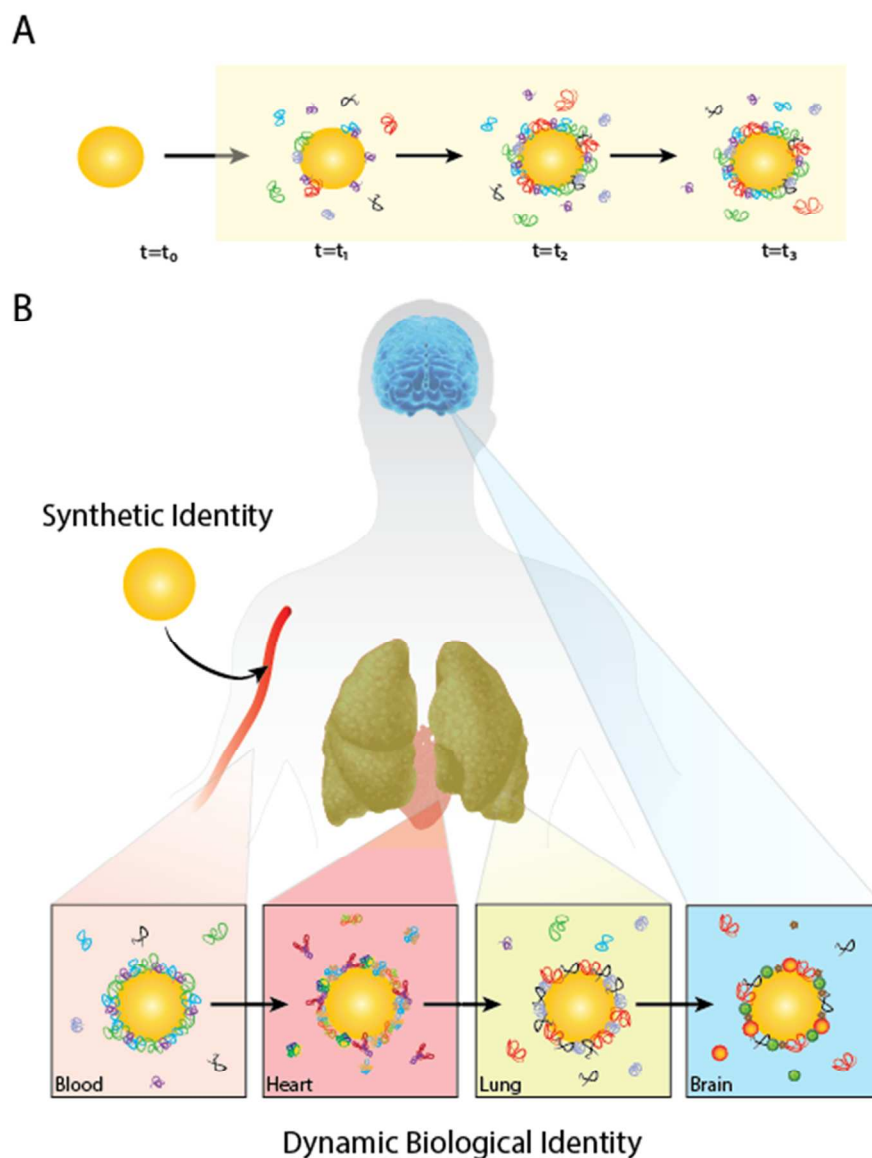


**Figure 3:** When pristine nanoparticles are exposed to a biological environment, proteins rapidly bind to the surface to form a protein corona. This converts the synthetic identity to a biological one. The nanoparticle physicochemical identity, exposure time and the local environment drive this process. A) In a static environment, the protein corona forms within minutes of exposure, and is composed of high abundance low affinity proteins. Over time, equilibrium is achieved when this soft corona is replaced by high affinity low abundance proteins to form a hard corona. B) In a dynamic environment, convection and cellular metabolism constantly change blood content, preventing an equilibrium composition from forming. When nanoparticles are injected intravenously, the protein corona that forms is related to location of administration and local environment. As it travels through the body, and nearby other organs, the unique cellular metabolism and proteins of each area constantly evolves the protein corona.

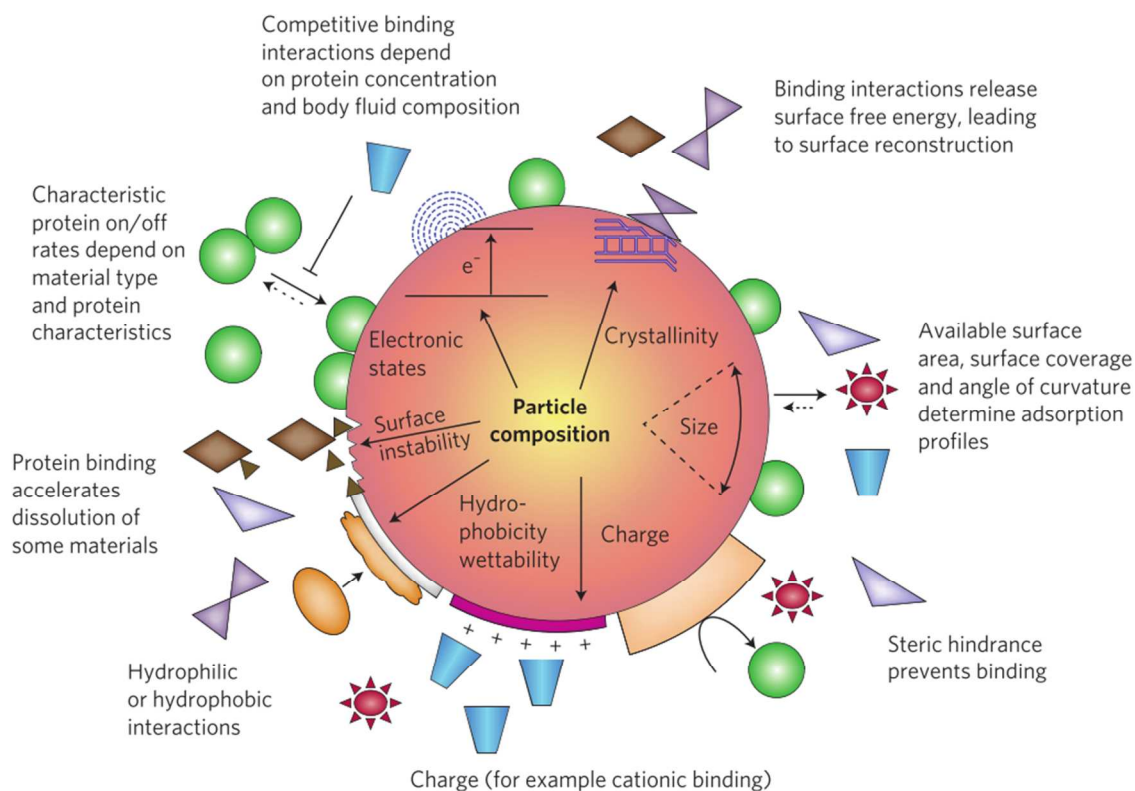


**Figure 4: Nanoparticle synthetic identity influences protein adsorption.** Nanoparticle physicochemical properties dictate interfacial interactions with proteins adsorbing to the surface and consequently nanoparticle fate. Material composition influences protein binding the greatest followed by surface chemistry and shape, other physical properties such as crystallinity, size, charge, hydrophobicity, surface instability, electronic states, surface roughness and radius of curvature also contribute in different ways to protein binding and corona formation and composition (figure taken from Nel *et al.* 2009 with permission)<sup>25</sup>.

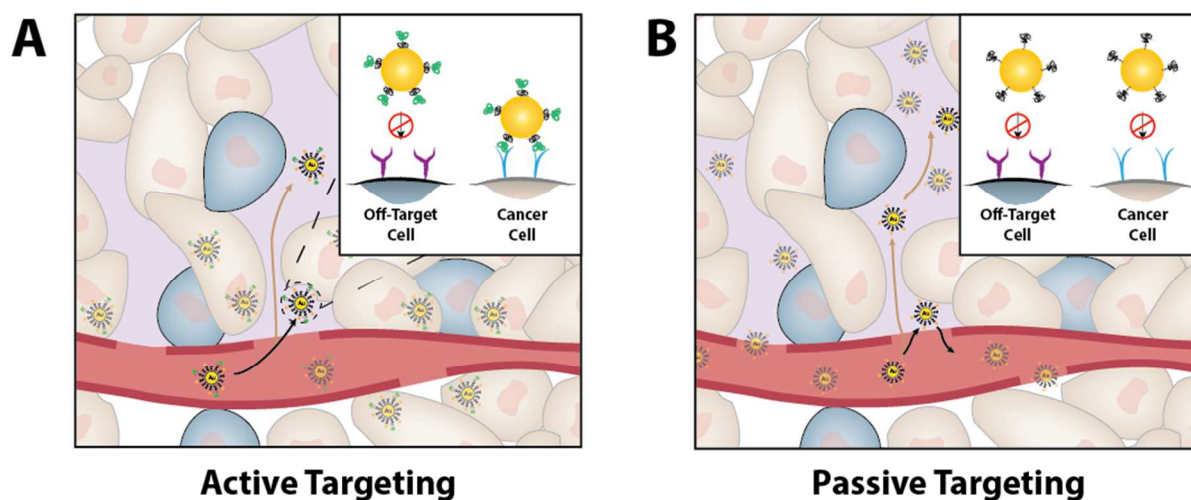
Particle type	Size (nm)	Surface Chemistry	Effect on Biological Identity	Source
Polystyrene	50	Bare	High Acute Phase and Ig proteins found in corona	Lundqvist 2008,2010
Polystyrene	50	Carboxyl Modified	High acute phase, low Ig, LDL/VLDL proteins found in corona	Lundqvist 2008,2010
Polystyrene	50	Amine Modified	High HDL, low Apo A-1, complement and Ig	Lundqvist 2008,2010
Polystyrene	100	Sulfonated	High HDL, low complement, hydrophobic surface favours protein binding	Monopoli, 2011
Polystyrene	200	Sulfonated	High Fib- $\alpha/\beta$	Monopoli, 2011
Polystyrene	80-110	NH <sub>2</sub> /NHR/NR <sub>2</sub> /NR <sub>3</sub> / COO <sup>-</sup> /SO <sub>3</sub> <sup>-</sup> /SO <sub>4</sub> <sup>2-</sup>	Increase surface charge density results in more protein binding to the surface (Pi>5.5 HIGH immune protein interaction/Pi<5.5 high albumin and lipoprotein)	Gessner, 2003
Polystyrene	250	Non-functionalized	High IgG and High Fibrinogen with Low Albumin and High Apolipoprotein	Gref, 2000
Polystyrene	250	ABA Block Co-Polymer (Poloxamer 407)	Low IgG and Low Fibrinogen with High Albumin and High Apolipoprotein	Gref, 2000
Polystyrene	60	Poloxamer (184/188/407)	Increase hydrophobicity increases the number of protein bound to the surface (IgG major)	Blunk, 1993
Fluorescent Polystyrene	40	NH <sub>2</sub>	Rapidly bind CS proteoglycans/anionic serum protein/bind scavenger receptor	Fleischer, 2012
Fluorescent Polystyrene	87	COOH	Bind native protein receptor/repel serum protein	Fleischer, 2012
Fluorescent Polystyrene	200	NH <sub>2</sub>	Rapidly bind CS proteoglycans/anionic serum protein/bind scavenger receptor	Fleischer, 2012
Fluorescent Polystyrene	200	COOH	Bind native protein receptor/repel serum protein	Fleischer, 2012
Silica	6	Bare	High Apo A-1 binding	Lundqvist 2010
Silica	50	Bare	High Apo A-1 binding	Monopoli, 2011
Silica	200	Bare	High Apo-1, serum albumin	Monopoli, 2011
Silica	50/100	NH <sub>2</sub> /COOH	Size had a greater effect on protein binding than charge	Zhang, 2011
Silica	15-165	Hydrophobic/ Hydrophilic	As radius of curvature increases, protein stability changes/Increase hydrophobicity protein molecules/particle increases	Roach, 2006
Amorphous Silica	9.6	Bare	High complement binding	Tenzer, 2011
Amorphous Silica	15.7	Bare	High lipoprotein binding	Tenzer, 2011
Amorphous Silica	54.9	Bare	Cellular component/Tissue leakage/Disease response	Tenzer, 2011
PMAPHOS-stat-PLMA-stat-PgMA)-Gold	15.8	NH <sub>3</sub> /Trimethyl Ammonium	High cell uptake	Huhn, 2012

Nanoparticle				
PTMAEMA-stat-PLMA-stat-PgMA-Gold Nanoparticle	10.2	Phosphonate/COOH	Forms small agglomerates	Huhn, 2012
Quantum Dot	4.4-8.7	DHLA/Cysteamine/Cysteine/DHLA-PEG	Changes corona size, biodistribution	Choi, 2007
50:50 Copolymer	70/200	NIPAM/BAM	HSA (LOW) HDL (HIGH) FIBRINOGEN (N/A) Packing density decreases as size increases or radius decreases  Increased Hydrophobicity increases surface packing density	Dell'Orco, 2010
Fe/Pt and CdSe/ZnS	10/20	COOH	Increase in particle radius was 3.3nm ~ thickness of structure to form a sphere	Rocker 2009
Gold	15/30/60/90	Methoxy PEG	As PEG concentration increases, protein family changes. High PEG elicits low complement and high immunoglobulin binding. Low PEG, however has high complement binding and low immunoglobulin	Walkey, 2012
Gold	10/60/200	Citrate/PEG	Curvature/surface chemistry/size	Benetti, 2013
Gold	4/10	(+) AUT (-) MUA	>10nm low protein adsorption/High radius of curvature <10nm High protein adsorption/Low radius of curvature	Casals, 2010
Gold	15/30/60	67 Surface Ligands (+/-n)	Results show that protein composition is influenced most by material composition then size then surface chemistry	Walkey, 2014
Gold	30	Citrate	Z-average diameter 76.1/after trypsin 49.6/more proteins bound to surface	Dobrovolskaia, 2009
Gold	50	Citrate	Z-average diameter 100/after trypsin 87.3/less proteins bound to surface	Dobrovolskaia, 2009
Gold	10/60/200	Citrate/PEG	Smaller particles bind greater number of blood protein	Benetti, 2013
Gold Nanorods	10X36	CTAB	Decrease surface curvature, increases protein binding	Gagner, 2011
Gold Nanospheres	10.6	CTAB	Decrease surface curvature, increases protein binding	Gagner, 2011
Gold	5-100	Citrate coated	Decrease surface curvature, changes protein conformation	Goy-López, 2012
Silver	24	Citrate/PVP	BSA had a lower binding affinity to electrostatically stabilized particles	Podila, 2012
Titanium Dioxide	20/200	Vitronectin coated	Reduced adsorption	Tedja, 2012
Iron Oxide	7-12.	TREG	High immunoglobulin and fibrinogen binding	Jansch, 2012
Oil-in-water emulsions	280	ABA Block Co-Polymer (Ploxamer 407)	High apolipoprotein binding	Harnisch, 2000

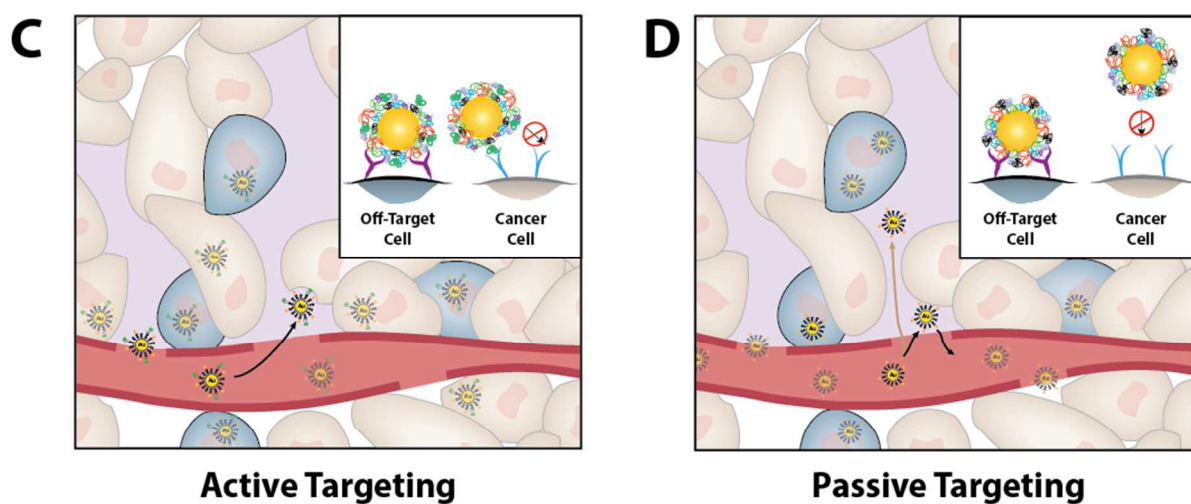
Liposome	102-109	(+) DOPE/Lipid-Cholesterol	High charge density (fibrinogen) and Low charge density (complement and immune proteins)	Capriotti, 2012
Liposome	96	(+) DOPE/Lipid	High apolipoprotein binding	Caracciolo, 2013
Liposome	223	(+) DOPE/Lipid-Cholesterol	High fibrinogen binding	Caracciolo, 2013
Spherical	100-200	Alumina/Silica/Latex	Interactions is reduced by surface roughness because the particle substrate interfacial separation is effectively larger rough surfaces more favourable for colloid deposition because of VDW	Hoek, 2007

**Table 1.** A list of the various nanoparticle physicochemical influences on protein adsorption and protein corona composition.

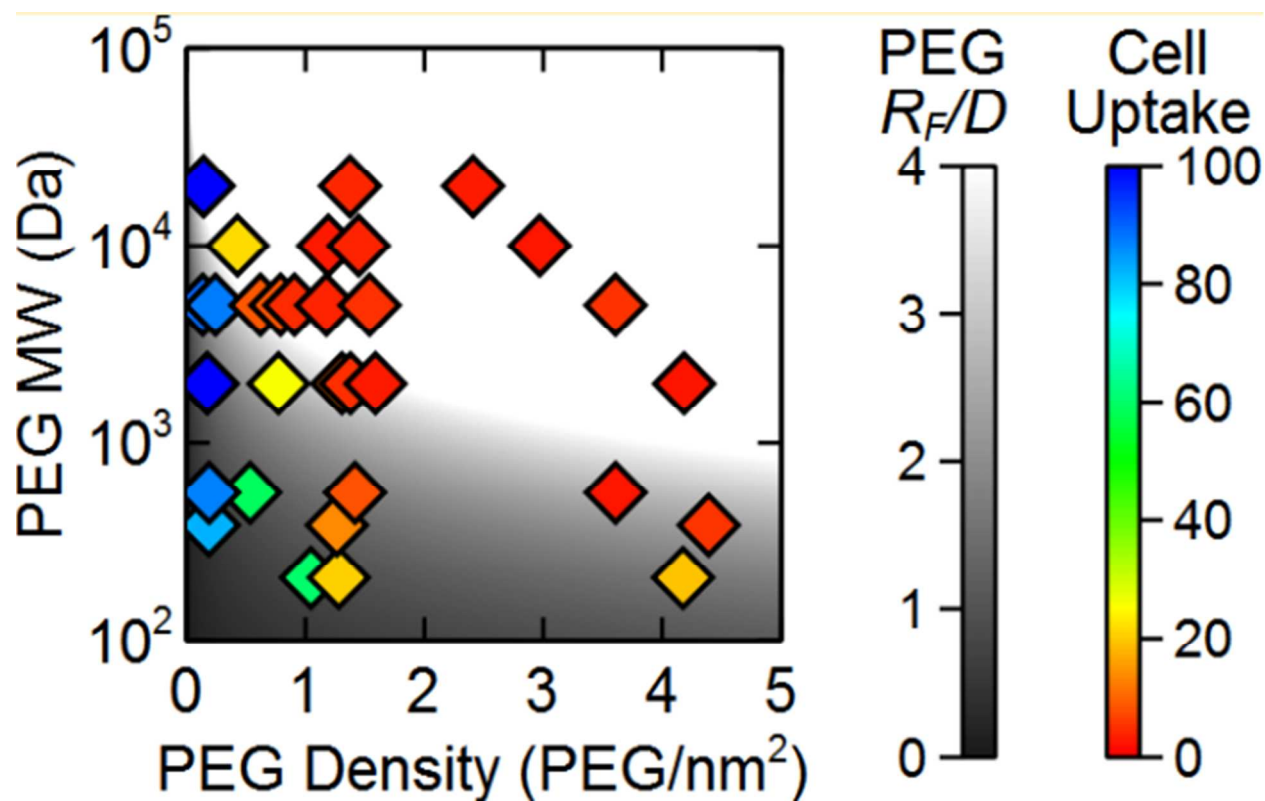
## Expected Outcome



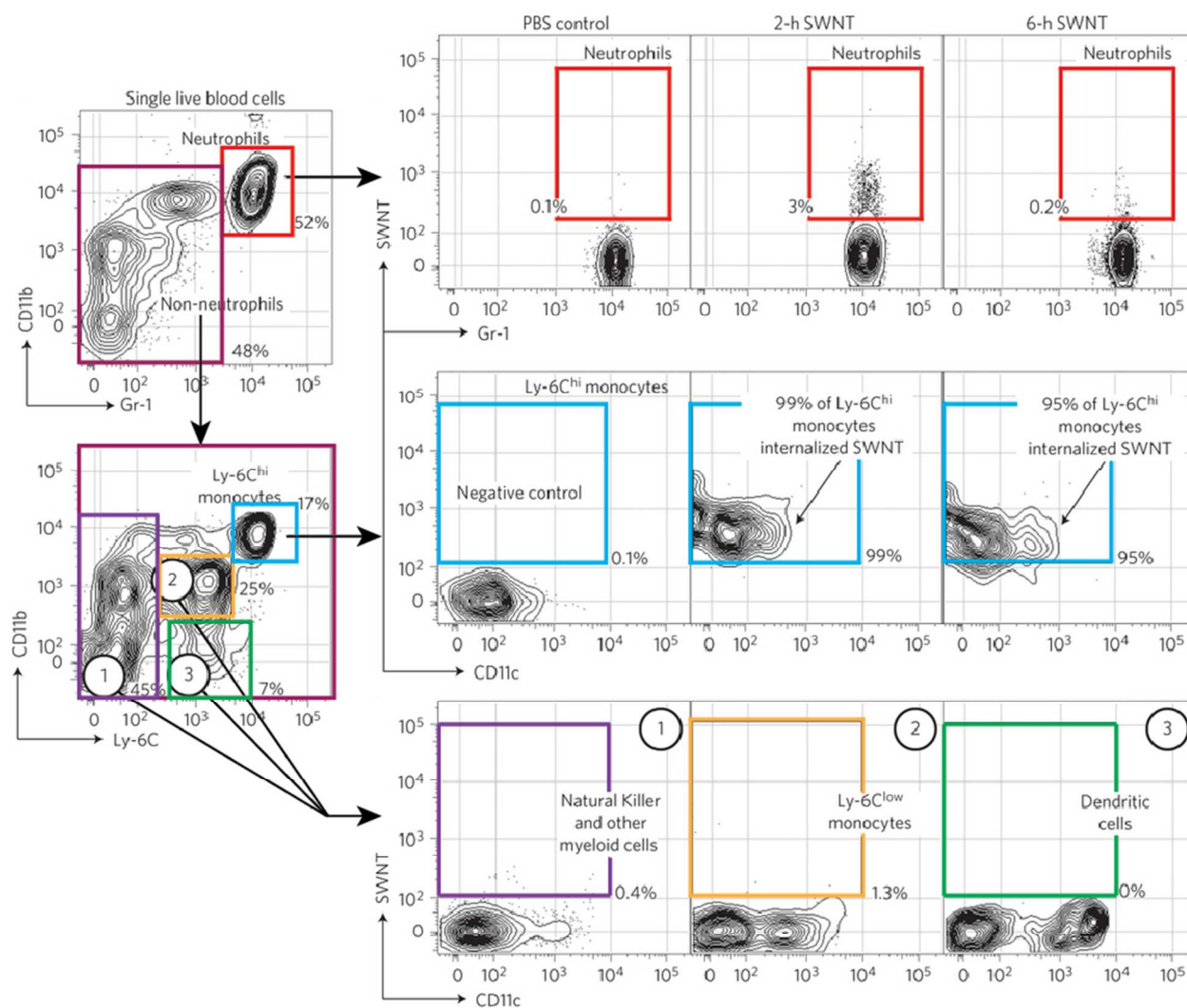
## True Outcome



**Figure 5: Ideal versus actual nanoparticle-tumour targeting strategies.** In tumours, the unique fenestrated vasculature facilitates nanoparticle extravasation from the blood and into the interstitium. The poor lymphatic drainage and high intratumoural pressure help retain the nanoparticles within the mass. In an ideal situation without nanoparticle-blood interactions: A) Nanoparticles are surface functionalized with ligands, to bind to cell surface receptors and undergo receptor mediated endocytosis for selective entry. B) Nanoparticles are surface passivated with PEG to increase half-life, and provide greater opportunity to extravasate through leaky tumour endothelium and penetrate tumour cells. *In vivo* nanoparticle-blood interactions cause protein corona formation and C) sterically hinders and masks surface bound ligands, limits cancer cell receptor mediated interactions and supports off-target effects. D) Nanoparticles increase in size, become more negative, and exhibit delayed diffusion kinetics, which limits extravasation through leaky tumour endothelium and contributes to off-target cell

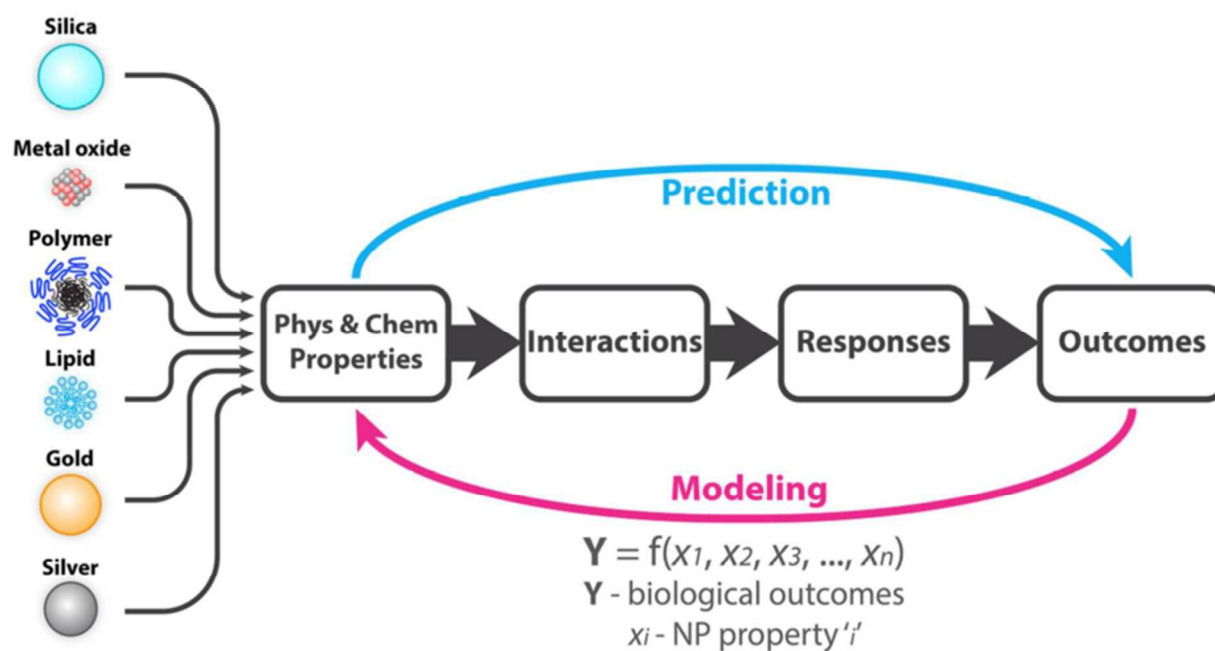


**Figure 6:** Different PEG molecules exhibit different optimal PEG densities on nanoparticle surfaces. At a specific PEG/nm<sup>2</sup> cell uptake is minimized (figure retrieved from Yang *et al.* 2014 with permission)<sup>67</sup>.



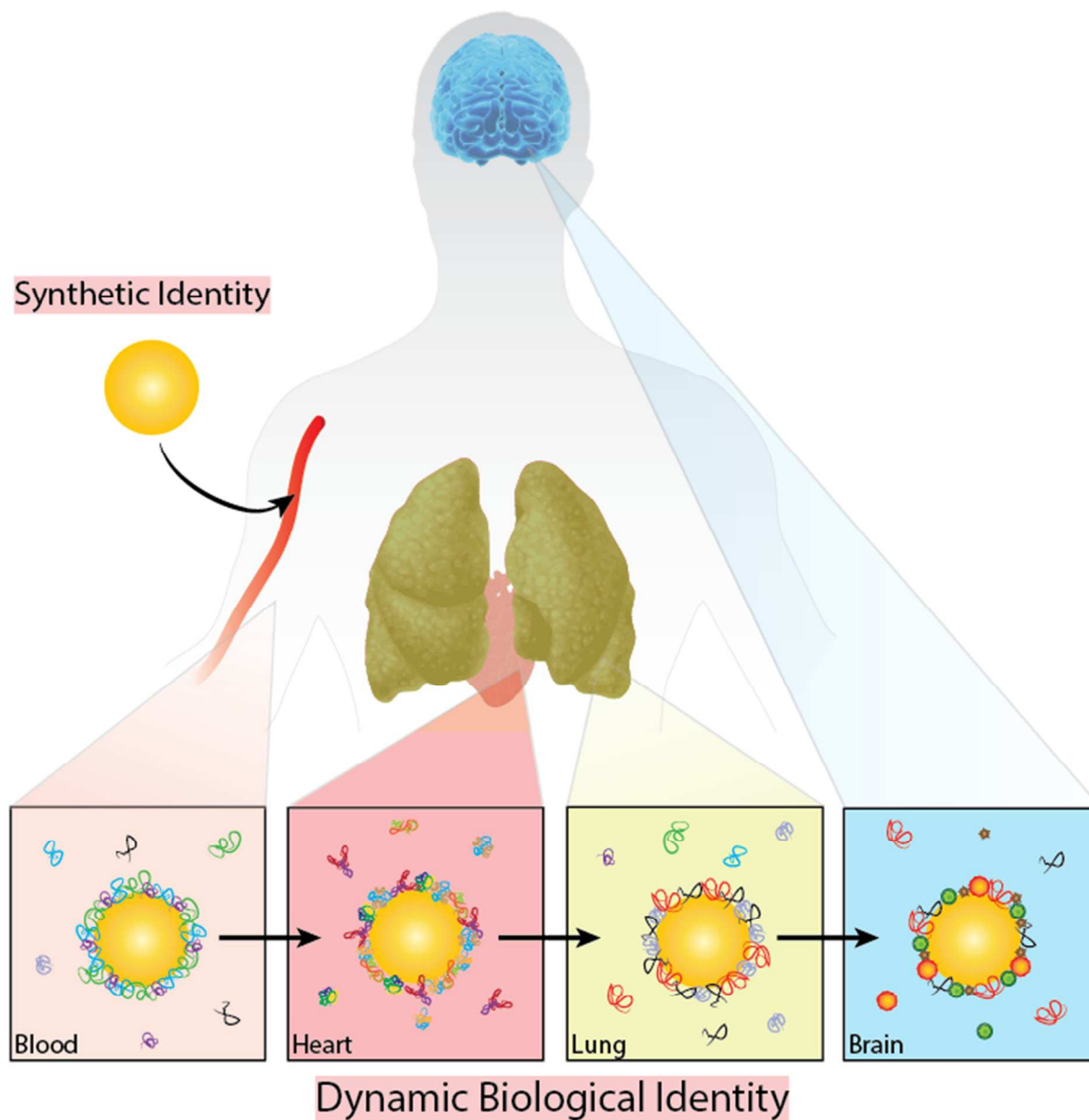
**Figure 7: Nanoparticle uptake in various blood cells.** Flow cytometry plots in the blood showing preferential uptake of SWNTs in neutrophils (RED) and non-neutrophil populations (MAUVE). Neutrophils, natural killer and other myeloid cells (PURPLE), Ly-6C<sup>low</sup> monocytes (YELLOW) and dendritic cells (GREEN) show minimal uptake, whereas Ly-6C<sup>high</sup> monocytes (BLUE) appear to show selective uptake (figure adapted from Smith *et al.* 2014 with permission)<sup>98</sup>.





**Figure 9: The design of QSAR models using nanoparticle libraries.** A variety of nanoparticle types can be processed similarly to Walkey *et al.* 2014. This model should provide perspective towards designing a library to evaluate nanoparticle physicochemical properties influence on protein binding, and how protein binding influences cellular interaction. Biological identity has a direct effect on cellular interaction<sup>42</sup>, and its effects can be simulated using computer modelling techniques. Evaluating biological outcomes to better design experiments and algorithms will advance cancer-nanomedicine (figure taken from Walkey *et al.* 2014 with permission)<sup>42</sup>.

## Table of Content Figure



This review examines nanoparticle-blood interactions, their implications on solid tumour targeting, and provides an outlook to guide future nanoparticle design.